25th ABCM International Congress of Mechanical Engineering
October 20-25, 2019, Uberlândia, MG, Brazil

COB-2019-1918
APPLICATION OF THE ADAPTATIVE HAMILTONIAN MONTE CARLO (AHMC) FOR FASTER CONVERGENCE IN THE ESTIMATION OF THERMAL PROPERTIES IN HOMOGENEOUS THIN PLATES

Maicon de Paiva Torres
Géssica Ramos da Silva
Diego Campos Knupp
Leonardo Tavares Stutz
Antônio José da Silva Neto
Polytechnic Institute, Rio de Janeiro State University – IPRJ/UERJ, Nova Friburgo/RJ - Brazil
mptorres@iprj.uerj.br, grsilva@iprj.uerj.br, diegoknupp@iprj.uerj.br, ltstutz@iprj.uerj.br, ajsneto@iprj.uerj.br

Abstract. *In this work, an adaptative version of the Markov Chain Monte Carlo method (MCMC) known as Hamiltonian Monte Carlo (HMC) is proposed to estimate the thermophysical properties of a thin plate made of a homogeneous material. The direct problem is based on the experimental setup for temperature nonintrusive measurements, in which the plate stands vertically whilst one surface is partially heated by an electric resistance and the other surface loses energy to the vicinity by radiation and natural convection. With regard to parameter space exploration, HMC stands in front of conventional random walk MCMC, such as Metropolis-Hastings algorithm, due to its deterministic explorative nature based on the gradient of the posterior distribution probability density, being more consistent and efficient. In order to enhance the Markov chains convergency for the inverse problem solution, an Adaptative Hamiltonian Monte Carlo (AHMC) version was implemented. On account of this adaptation, it is possible to control the acceptance rate to a desirable level and achieve more stable solutions.*

Keywords: *Heat conduction, Lumped formulation, Thermophysical properties estimation, Adaptative Hamiltonian Monte Carlo*

1. INTRODUCTION

Heat conduction problems are commonly applied in the determination of thermal properties of materials (Knupp et al., 2013) and (Wang et al., 2019). For instance, the non-homogeneous materials development industry, such as nanocomposites, deals with the problem of having to characterize the physical properties of its products on a case-by-case basis in order to guarantee its efficiency in use. This is due to the innumerable possibilities of composition and arrangement, inherent to the productive process (Danes et al., 2003) and (Kumlutas and Tavman, 2006).

Having a probabilistic model for the observed data, through Bayesian inference it is possible to adequately quantify the uncertainties and obtain the global structure of the parameter space (Kaipio and Somersalo, 2004). In most engineering problems, Bayes' theorem cannot be solved analytically, necessitating efficient integration techniques.

The Metropolis-Hastings algorithm (MH) (Metropolis et al., 1953) is considered the simplest and one of the most used among the Markov chain Monte Carlo methods (MCMC). However, successive states may have high correlation due to the random nature of the movement in the space of the parameters. As a result, the effective size of the sample tends to be small. In order to overcome the inefficiency of random walking MCMC methods, Duane et al. (1987) proposed in their work the Hamiltonian Monte Carlo method (HMC), which contains a deterministic mechanism inspired by the Hamiltonian dynamics to propose samples for the target probability distribution (Neal, 2011).

This work is based in the application of an adaptative version of the HMC, known as Adaptative Hamiltonian Monte Carlo (AHMC) (Boulkaibet et al., 2016). Despite the advantages of the HMC compared to random walk MCMC methods (Kumar et al., 2017), (Torres et al., 2018a,b), the AHMC allows one to perform a more efficient and consistent search in the parameters space whilst guarantee the simulation stability following a reference acceptance rate stablished previously. Another advantage registered through the simulations with the AHMC is the possibility the system has to automatically update the parameters of the numerical integration (leapfrog method), allowing a faster convergency in the Markov chains. It was checked by performing a modification in the adaptation proposed in the work of Boulkaibet et al., (2016), where the parameters updating variates at different levels, interfering towards in the inverse problem convergence.

2. DIRECT PROBLEM FORMULATION AND SOLUTION

Consider a heat transfer problem based on a plate subjected to a prescribed heat flux at one face and convective and radiative heat losses at the opposite face (see Fig. 1). As the heating element has the same width as the sample plate (40 x 40 mm) neglecting the temperature gradients on the width direction y is plausible and then is possible to construct the potential $T(x,z,t)$ in the region $x \in [0, L_x]$ and $z \in [0, L_z]$. This problem can be formulated by Eqs. (1a-f), which consists of the homogeneous version of the bi-dimensional transient heat conduction formulation presented in (Knupp et al., 2012)

$$w\frac{\partial T(x,z,t)}{\partial t} = k\frac{\partial^2 T(x,z,t)}{\partial x^2} + k\frac{\partial^2 T(x,z,t)}{\partial z^2}, \quad 0 < x < L_x, \quad 0 < z < L_z, \quad t > 0 \tag{1a}$$

$$T(x,z,0) = T_\infty, \quad 0 \le x \le L_x, \quad 0 \le z \le L_z \tag{1b}$$

$$\left.\frac{\partial T(x,z,t)}{\partial x}\right|_{x=0} = 0, \quad \left.\frac{\partial T(x,z,t)}{\partial x}\right|_{x=L_x} = 0, \quad t > 0 \tag{1c,d}$$

$$-k\left.\frac{\partial T(x,z,t)}{\partial z}\right|_{z=0} = q''(x), \quad k\left.\frac{\partial T(x,z,t)}{\partial z}\right|_{z=L_z} + h(x)T(x,L_z,t) = h(x)T_\infty, \quad t > 0 \tag{1e,f}$$

The equation coefficients w and k are, respectively, the volumetric heat capacity [J/m³K] and the thermal conductivity [W/mK], that forms the concerned thermophysical properties to be estimated in the inverse problem.

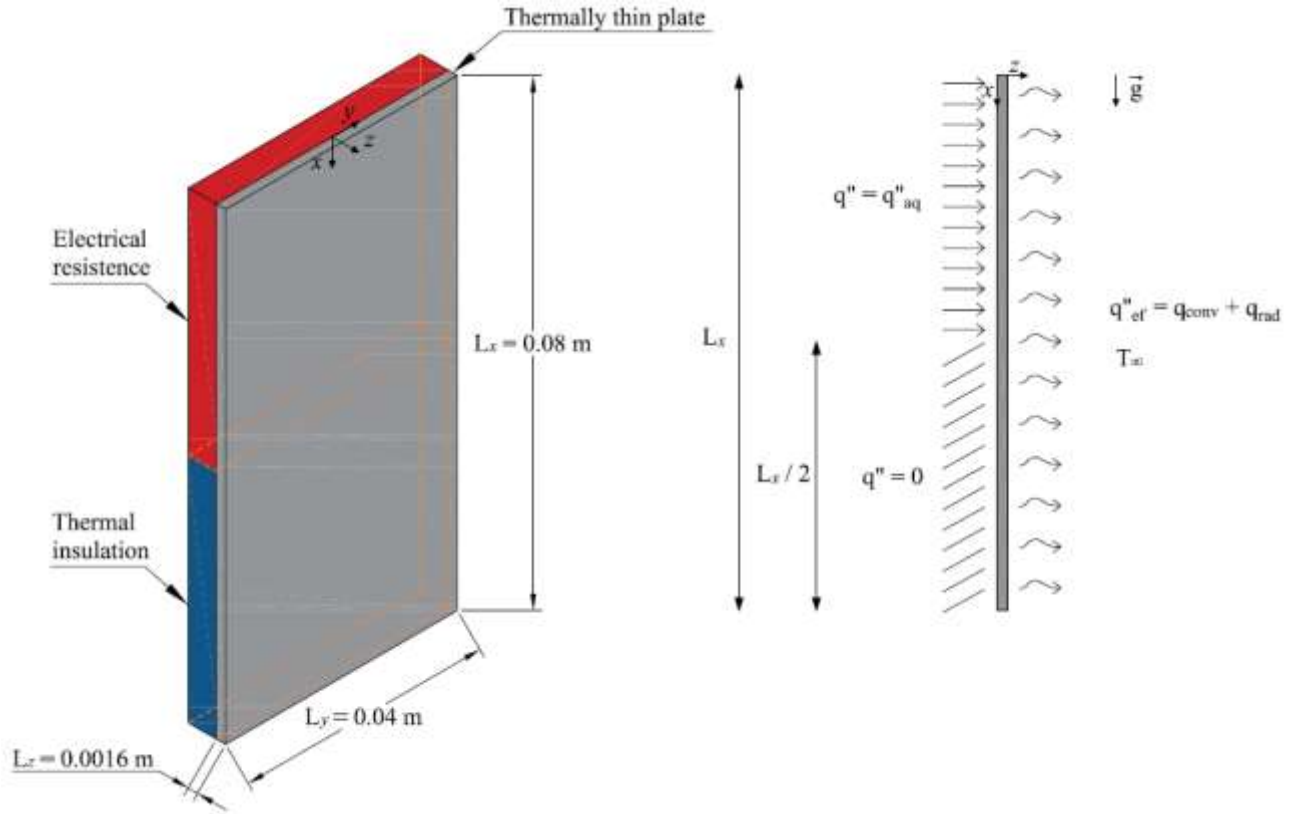

Figure 1. Configuration of the thermally thin plate with the schematic representation of the heat transfer process.

Assuming that the plate is thermally thin, a straightforward lumped formulation can be considered across the sample thickness, as proposed in (Neveira-Cotta et al., 2011) with the definition of the average temperature across the z direction for the transversally averaged temperature field in the x and z directions

$$T_m(x,t) = \frac{1}{L_z}\int_0^{L_z} T(x,z,t)dz \tag{2}$$

The new formulation includes the transient term, the diffusion operator, a linear dissipation term, and an independent source term, $P(x)$. The heat conduction equation with the corresponding initial and boundary conditions are given by

$$w\frac{\partial T_m(x,t)}{\partial t} = k\frac{\partial^2 T_m(x,t)}{\partial x^2} - d(x)T_m(x,t) + P(x), \quad 0 < x < L_x, \quad t > 0 \tag{3a}$$

$$T_m(x,0) = T_\infty, \quad 0 \le x \le L_x \tag{3b}$$

$$\left.\frac{\partial T_m(x,t)}{\partial x}\right|_{x=0} = 0, \quad \left.\frac{\partial T_m(x,t)}{\partial x}\right|_{x=L_x} = 0, \quad t > 0 \tag{3c,d}$$

where

$$d(x) = \frac{h_{ef}(x)}{L_z} \tag{3e}$$

$$P(x) = \frac{q''(x)}{L_z} + \frac{h_{ef}(x)}{L_z}T_\infty \tag{3f}$$

Equations (3a-f) models a typical one-dimensional transient thermal conduction problem in a homogeneous thermally thin plate, including prescribed heat flux at one face, and convective and radiative heat losses at the opposite face. The resistance has the dimensions 0,04 x 0,04 m in the x and y directions, and is attached to its superior half, whereas the inferior portion of this surface is thermally insulated. In this configuration, the heat flux, $q''(x)$, along the x direction, is modeled as

$$q''(x) = \begin{cases} q''_{aq}, & 0 \le x \le L_x/2 \\ 0, & L_x/2 < x \le L_x \end{cases} \tag{4}$$

where q''_{aq} = 440,5 W/m² is the power directed from the electrical resistance into the plate.

The effective heat transfer coefficient, $h_{ef}(x)$, takes into consideration the heat losses from the plate to the environment, at temperature T_∞ = 24 °C, considering natural convection over vertical plates and linearization of the radiative heat flux to the vicinity at the same temperature T_∞. Taking into account the different temperatures at the heated and unheated plate portions, the effective heat transfer coefficient can also be described by the step function

$$h(x) = \begin{cases} h_{x0}, & 0 \le x \le L_x/2 \\ h_{xL}, & L_x/2 < x \le L_x \end{cases} \tag{5}$$

where h_{x0} is 17,0 W/m²K and h_{xL} is 4,0 W/m²K.

After all mathematical model coefficients have been defined, the formal solution for problem (3) is obtained via an explicit Finite Difference Method (FDM). A convergency study was carried out and the temperature distributions were determined through the appropriate chosen computational grid.

3. INVERSE PROBLEM FORMULATION AND SOLUTION

In the Bayesian approach, all possible information is incorporated to the model in order to reduce the degree of uncertainty present in the experimental data. Assuming that some prior information with respect to the parameters vector $Z^T = [w, k]$ is available, the information can be modeled as a probability density $\pi(Z)$, and the Bayes' theorem for inverse problems can be expressed by

$$\pi_{posterior}(Z) = \pi(Z \mid Y) = \frac{\pi(Z)\pi(Y \mid Z)}{\pi(Y)} \tag{6}$$

where $\pi(Z \mid Y)$ is the posterior probability density, $\pi(Z)$ is the prior probability density, $\pi(Y \mid Z)$ is the likelihood function, and $\pi(Y)$ is the marginal probability density, which is a normalization constant.

Assuming the synthetic experimental errors are random variables with Gaussian distribution, with zero mean and known covariance matrix W, besides being additive and independent of the parameters Z, the likelihood function can be written as

$$\pi(Y \mid Z) = (2\pi)^{-Nd/2} |W|^{-1/2} \exp\left[-\frac{1}{2}(Y - T(Z))^T W^{-1} (Y - T(Z)) \right] \tag{7}$$

where $T(Z)$ is the solution of the direct model, and N_d is the number of experimental measurements.

3.2 Hamiltonian Monte Carlo method (HMC)

The first step to construct the MCMC method with the Hamiltonian dynamics is to define a Hamiltonian function in terms of the target probability distribution to be sampled of. In addition to the variables of interest w and k (seen now as position variables), it is necessary to introduce momentum variables, which often have independent Gaussian distributions. For each parameter Z_i, an associated momentum variable, p_i, is introduced. The Hamiltonian H is then constructed by considering the sum of a potential energy term, $U(Z)$, with a kinetic energy term, $K(p)$, in the form

$$H(Z, p) = U(Z) + K(p) \tag{8}$$

where $U(Z)$ is the negative of the posterior probability distribution logarithm, given by $U(Z) = -\ln(\pi(Z \mid Y))$, and $K(p)$ is the kinetic energy, defined as

$$K(p) = \frac{1}{2} p^T \overline{M}^{-1} p \tag{9}$$

where $\overline{M}$ is the mass matrix, symmetric and positive-definite, which is typically diagonal. This form for $K(p)$ corresponds to the negative of the probability density logarithm (plus a constant) of a Gaussian distribution with zero mean and covariance matrix $\overline{M}$.

The partial derivatives of the Hamiltonian determine the way Z and p change over time, t, according to the following equations

$$\frac{dZ}{dt} = \frac{\partial H}{\partial p}, \quad \frac{dp}{dt} = -\frac{\partial H}{\partial Z} \tag{10a,b}$$

Each iteration of the algorithm begins with a sampling to generate new momentum variables from the Gaussian distribution given by the kinetic energy. Consequently, the trajectory in the state space (Z, p), which must keep H

constant, is traced by the leapfrog numerical integration technique, which depends on the number of steps, L, and the step size, ε. For L = 1, we have the following steps for the integration of the movement equations (10a,b)

$$p(t+\varepsilon/2) = p(t) - (\varepsilon/2)\frac{\partial U(Z(t))}{\partial Z} \tag{11a}$$

$$Z(t+\varepsilon) = Z(t) + \varepsilon \overline{M}^{-1} p(t+\varepsilon/2) \tag{11b}$$

$$p(t+\varepsilon) = p(t+\varepsilon/2) - (\varepsilon/2)\frac{\partial U(Z(t+\varepsilon))}{\partial Z} \tag{11c}$$

where the potential energy gradient is obtained, in this work, with a finite difference approximation.

Momentum variables have the signals exchanged at the end of the trajectory in order to make the Metropolis proposal symmetrical. Considering the Hastings ratio,

$$\alpha_{HMC} = \min\left[1, \exp\left(-H(Z^*, p^*) + H(Z^*, p^*)\right)\right] \tag{12}$$

and a random value θ', generated from a uniform distribution in the interval $(0,1)$, the proposed state (Z^*, p^*) is accepted, if $\theta' < \alpha_{HMC}$, as a new state in the Markov chain with probability α_{HMC}. Otherwise it is rejected.

3.3 Adaptative Hamiltonian Monte Carlo method (HMC)

The Adaptative Hamiltonian Monte Carlo method was proposed in the work Boulkaibet et al (2016). The method consists of an adaptative version of the HMC and allows a more efficient sampling in the posterior probability distribution (the parameters space). This is possible due the trajectory length adaptation to obtain sufficient large time steps whilst preserving the acceptance rate (calculate in the Hastings ratio) in a desirable level.

In this formulation, the number of steps for the time integration changes along the Markov chains states. Its value is sampled from a uniform distribution in the interval $[1, L_{\max}]$, where $L_{\max}$ = 5. In addition, initial value for the time step, ε, is also chosen from a uniform distribution, within the range $[\varepsilon_{\min}, \varepsilon_{\max}]$. In the current work, $\varepsilon_{\min}$ = 10^{-4} e $\varepsilon_{\max}$ = 10^{-3}, and the time step is updated at each 5 states.

In this way, the samples generated along the Markov chains evolution are employed to calculate the acceptance rate $\overline{\alpha}^{b}$, and depending on its result, the time step might increase or decrease, according to the following condition

$$\varepsilon^{i+1} = \begin{cases} \varepsilon^i + a\gamma^i\varepsilon^i, & \overline{\alpha}^{b} \geq \overline{\alpha} \\ \varepsilon^i - b\gamma^i\varepsilon^i, & \overline{\alpha}^{b} < \overline{\alpha} \end{cases} \tag{13}$$

where γ^i is a random variable selected in the interval [0.01; 0.05] and $\overline{\alpha}$ is the desirable acceptance rate.

4. RESULTS AND DISCUSSION

The thermally thin plate chosen for the inverse analysis performed in this work is made of a polyester resign. According to the literature, the exact values for the volumetric heat capacity and thermal conductivity may vary in the ranges [1.22-1.76] x 10^6 J/m³K and [0.15-0.17] W/mK, respectively (Mark, 2007). In this work, the exact values considered for the parameters w and k are 1.49 x 10^6 J/m³K and 0.16 W/mK, respectively.

Assuming the only prior information available for the material is that it belongs to the polymers class, it is found that their thermal conductivity is between 0.06 and 0.5 W/mK and the volumetric heat capacity may assume any value between 0.7x10^6 and 5.0x10^6 J/m³K. Thus, the prior information can be modeled as a bivariate uniform distribution whose bounds correspond to the upper and lower of the possible values for the parameters w and k.

It is not used real experimental data in this work and thereby synthetic data are generated by the addition of a noisy signal, with a controlled level, in the numerical solution of the direct problem, according to

$$Y_i = T_i\left(Z_{exact}\right) + \sigma e_i\,, \quad i = 1,2,...,N_d \tag{14a}$$

where $T_i\left(Z_{exact}\right)$ corresponds to the calculated values for the temperature using the exact values for the unknown parameters, Z_{exact}. e_i is a random number generated from a normal distribution with zero mean and unit standard deviation, and σ represents the standard deviation of the experimental data. The noise level is conveniently calculated by the expression

$$Noise(\%) = \max\left|\frac{\sigma e_i}{T_i\left(Z_{exact}\right)}\right| 100\%\,, \quad i = 1,2,...,N_d \tag{14b}$$

Although HMC demands a higher computational effort than Metropolis-Hastings algorithm to do the calculations, it still shows to be advantageous. The following results were generated considering 1000 states for the Markov chains, whose steady distribution allows one to perform the statistical inference to obtain the estimates (mean values) and their corresponding standard deviations (to account the uncertainty present in the experimental data). In Fig. 2 are presented the results depicted by a simulation performed via HMC, which is considered the first case (case 1). For these results it was adopted 5 time steps (L = 5) for the leapfrog integration scheme with 10^{-3} step length (ε = 10^{-3}). In light of convergency and numerical accuracy, a too high time step might imply to errors related to the discretization and, in this case, the higher are the number of steps, the faster these errors would propagate. On the other hand, too small time steps would decrease the solution convergency. Figure 2(a) shows the pathway covered in the parameters space during HMC simulation. One may note the fast convergency in the beginning, with a progressive slowdown until the target distribution be reached. It is acceptable, as the potential energy depends directly of the likelihood function, that decreases as the simulation advances. Figure 2(b) depicts the parameters dispersion and histograms. Although some systematic error is noticed, the dispersion presents small random errors, though the measurements uncertainties.

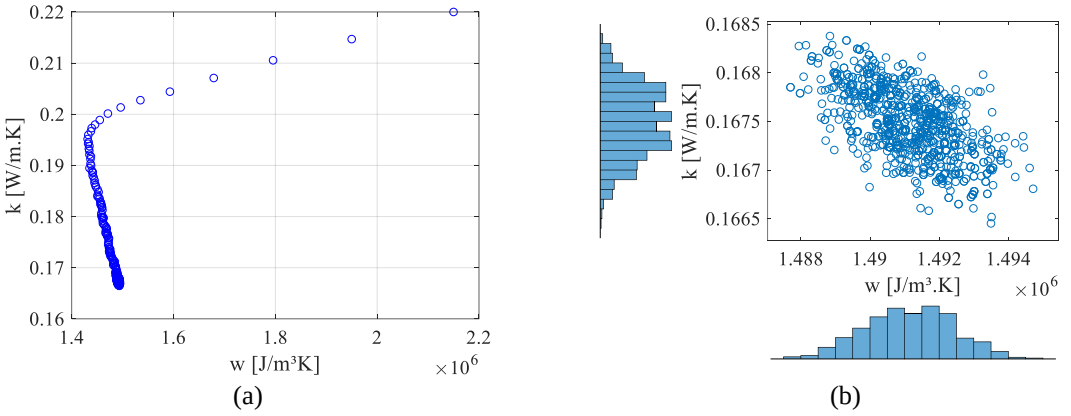

Figure 2. (a) Pathway covered in the parameters space by simulation performed via HMC. (b) Parameters dispersion discarding 150 states for heating the Markov chains (1000 states in total).

The Markov chains autocorrelations are presented in Fig. 3. By definition, in a Markov chain, a given state depends exclusively on the previous one. For this reason, we adopted a state delay (lag) of one state. Both Figs. 3(a-b) presents low autocorrelation levels for w and k chains, respectively. One may notice just a light autocorrelation for w chains, that may be caused due sensibility issues in the direct model formulation.

In order to carry out simulations with the AHMC, it was adopted $\overline{\alpha}$ = 80% and different values for the constants a and b, to investigate its effect on the HMC convergence. In the second case studied (case 2), it is considered the base case, carried out in the Boukaibet work (Boukaibet et al., 2016), where a = b = 1. Case 3 consider the least conservative scenario, forcing the convergency adopting a = 5 and b = 1. Finally, in the fourth case (case 4), it is presented the most conservative case. For this purpose, it is adopted a = 1 and b = 5, forcing the walk to slowdown for the system recover its stability.

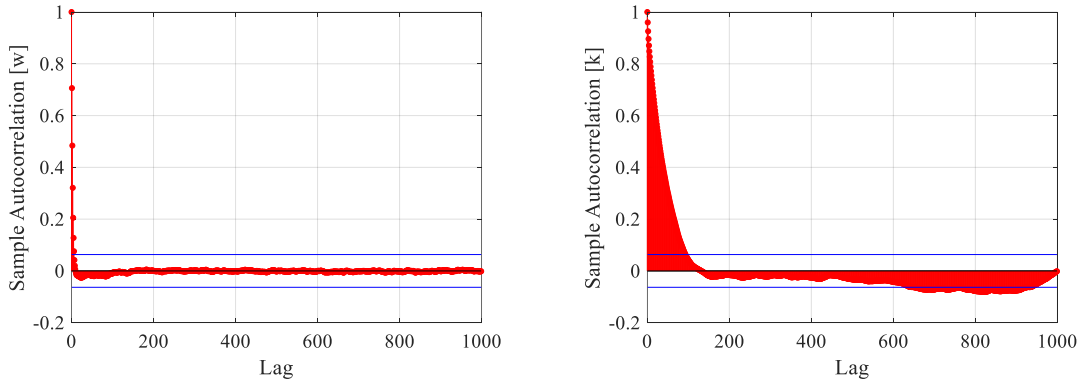

Figure 3. Markov chains autocorrelation functions considering one state delay (lag) and 1000 states for (a) w and (b) k.

Figure 4 presents the results for case 2. Figs. 4(a,b) shows the Markov chains for w and k, respectively. 500 states were necessary to achieve the stationary distribution. The variation of the step size ε is presented in Fig. 4(c). It is possible to observe a fairly balance of ε along the states. The highest value, $1.6\text{x}10^{-3}$, is reached when the chains reach the convergency. From this state on, this value tends to decrease, what helps to obtain posterior distributions with smaller random errors and smaller autocorrelation.

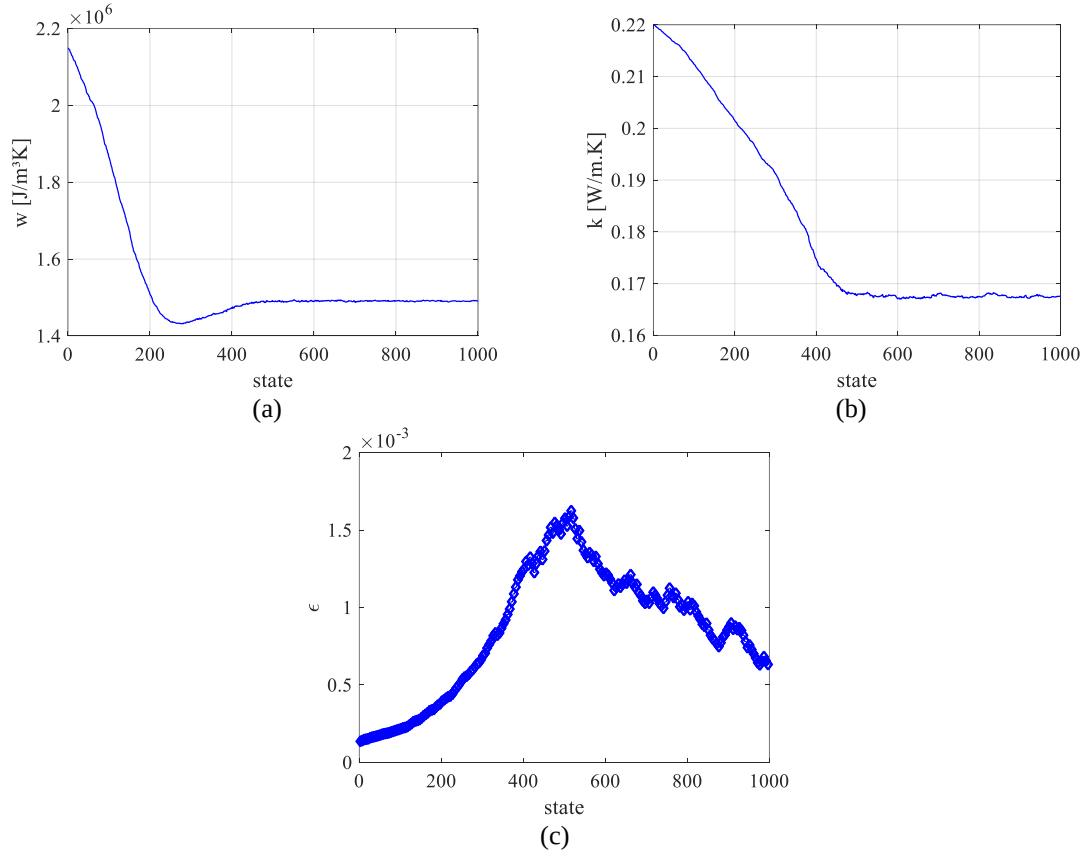

Figure 4. Markov chain for the parameters (a) w, (b) k and evolution of the time step (c) ε. It is considered 1000 states and surrogate temperature with 3% noise level for the base case (a=b=1).

Case 3 results are presented in Fig. 5. Through Figs. 5(a,b), one can figure it out the Markov chains convergency were faster than occurred in the previous case, being necessary just 180 states to reach the steady distribution. It was expected, since we have now the least conservative case in which the convergency is forced. Another advantage in this case is the high value achieved for ε ($3.4\text{x}10^{-3}$ in the 180th estate). However, it is possible to observe, in Fig. 5(c), certain degree of instability in the step size evolution.

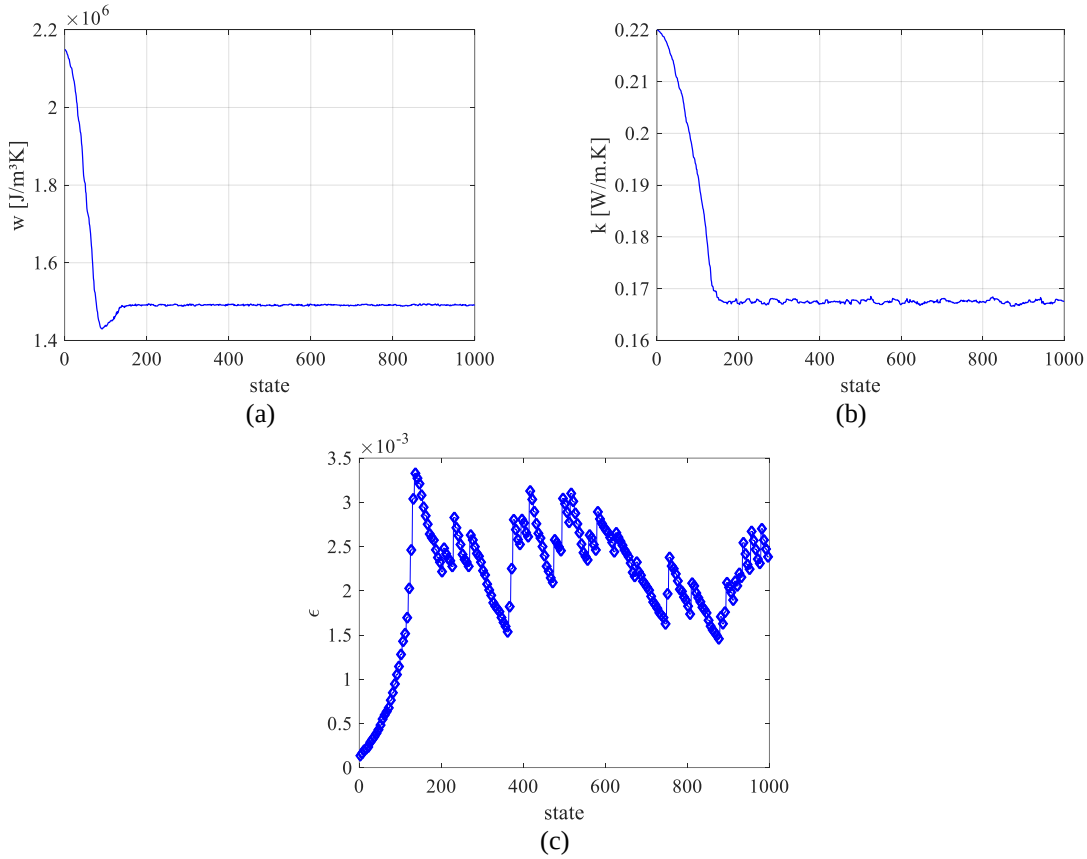

Figure 5. Markov chain for the parameters (a) w, (b) k and evolution of the time step (c) ε. It is considered 1000 states and surrogate temperature with 3% noise level for the least conservative case (a = 5 and b = 1).

In the final case (case 4), that represents the most conservative case, it was expected a slow convergency for the Markov chains, as shown in Figs. 6(a,b). As for the case 2, it was necessary about 500 states to reach the steady distribution. From the point of convergency, it is possible to conclude that there is no significant difference between cases 2 and 4. One may observe, in Fig. 6(c), that after achieve the convergency, there is an accentuate slope for decreasing the time step ε and the maximum value achieved was $1.2\text{x}10^{-3}$ at the 405^{th} state.

All cases presented previously are summed up in Tab. 1. In this table are depicted the estimates (means), standard deviations and acceptance rates for each case. It is clear that good estimates were achieved for all regarded cases. Special attention must be given for the standard deviations and acceptance rates. The posterior distributions that shown the smallest standard deviations were generated in cases 2 and 4. After reaching the steady distribution, the step sizes were considerably decreased, contributing for the system stability and, as consequence, smaller uncertainty is attributed.

In addition, cases 2 and 4 presented the highest values for the acceptance rates, 84.2% and 95.9%, respectively. Although the slow Markov chains convergency, the posterior distributions contain more effective samples, as fewer samples are repeated. Case 3, the least conservative, presented the highest standard deviations. As seen in Fig. 5(c), the time step evolution presented certain degree of instability during the Markov chain steady portion, assuming high values during the simulation. This interfered directly in the results uncertainty. However, its convergency was the fast among all cases, despite the low acceptance rate, 65,9%. Finally, it is important to highlight the similarities in the results presented by the cases 1 and 3. Their posterior distributions have close standard deviations and acceptance rates, though case 3 presented smaller computational effort due to the variable number of steps.

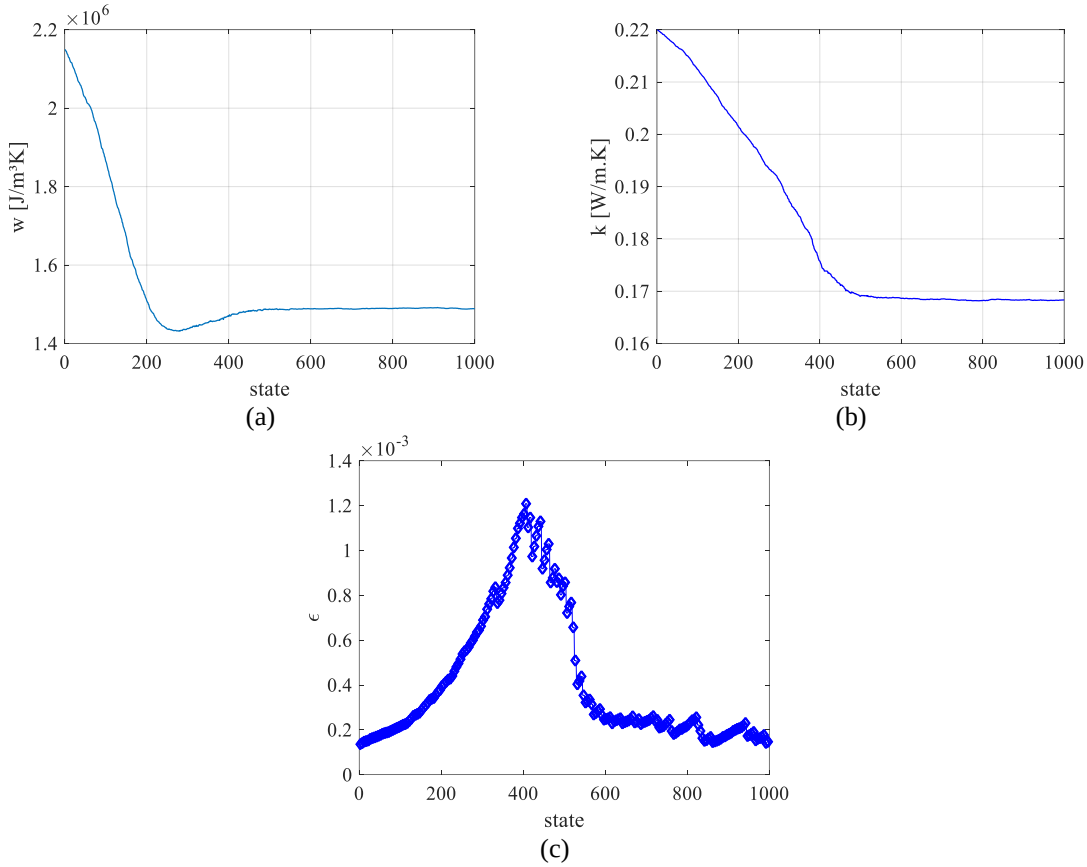

Figure 6. Markov chain for the parameters (a) w, (b) k and evolution of the time step (c) ε. It is considered 1000 states and surrogate temperature with 3% noise level for the most conservative case (a = 1 and b = 5).

Table 1. Estimated values, standard deviations and acceptance rates for the regarded cases. It was considered Markov chains with 1000 states and surrogate temperatures with 3% of noise level.

Case	MCMC	Property	Estimated	Standard deviation	Acceptance rate (%)
1	HMC $L = 5$; $\varepsilon = 0.001$	w [J/m³K]	1.4911×10^6	1.27×10^3	72.4
		k [W/mK]	0,1674	0.35×10^{-3}	
2	AHMC a = 1; b = 1	w [J/m³K]	1.4908×10^6	1.10×10^3	84.2
		k [W/mK]	0.1675	0.27×10^{-3}	
3	AHMC a = 5; b = 1	w [J/m³K]	1.4910×10^6	3.32×10^3	65.9
		k [W/mK]	0.1674	0.32×10^{-3}	
4	AHMC a = 1; b = 5	w [J/m³K]	1.4890×10^6	1.17×10^3	95.9
		k [W/mK]	0.1684	0.23×10^{-3}	

5. CONCLUSIONS

The present work considered the Adaptative Hamiltonian Monte Carlo for the thermophysical properties estimation of a thermally thin plate. A simple modification of the AHMC allowed to perform a convergency study of the Markov chains and to check its influence on the acceptance rate. It was shown that forcing the convergency may have some disadvantages, such as low acceptance rates and posterior probabilities distributions with high standard deviations, *i.e.*, high random errors. In the most conservative case, it was possible to observe a decrease in the posterior distribution spreadness (low standard deviation) and keep the acceptance rates above the desirable value. In addition, the most conservative AHMC case might be advantageous in comparison to the conventional HMC, when computational effort is

the matter. With a mean value calculated of 3 times steps per state, AHMC was able to achieve a similar convergency to the HMC with a fixed value of 5 time steps per state.

6. ACKNOWLEDGEMENTS

This study was financed in part by the Coordenação de Aperfeiçoamento de Pessoal de Nível Superior - Brasil (CAPES) - Finance Code 001.

The authors also acknowledge the financial support provided by FAPERJ – Fundação Carlos Chagas Filho de Amparo à Pesquisa do Estado do Rio de Janeiro and CNPq – Conselho Nacional de Desenvolvimento Científico e Tecnológico.

7. REFERENCES

Boulkaibet, I., Marwala, T., Friswell, M. I., & Adhikari, S. (2016). An adaptive markov chain monte carlo method for bayesian finite element model updating. In *Special Topics in Structural Dynamics, Volume 6* (pp. 55-65). Springer, Cham.

Danes, F., Garnier, B., & Dupuis, T. (2003). Predicting, measuring, and tailoring the transverse thermal conductivity of composites from polymer matrix and metal filler. *International journal of thermophysics*, *24*(3), 771-784.

Duane, S., Kennedy, A. D., Pendleton, B. J., & Roweth, D. (1987). Hybrid Monte Carlo. *Physics letters B*, *195*(2), 216-222.

Kaipio, J. P., & Somersalo, E. (2004). Computational and statistical methods for inverse problems. *Applied mathematical sciences*, *160*.

Knupp, D. C., Naveira-Cotta, C. P., Orlande, H. R., & Cotta, R. M. (2013). Experimental identification of thermophysical properties in heterogeneous materials with integral transformation of temperature measurements from infrared thermography. *Experimental Heat Transfer*, *26*(1), 1-25.

Kumar, S. R., Reddy, B. K., & Balaji, C. (2017). Application of Hybrid Monte Carlo Algorithm in Heat Transfer. Journal of Heat Transfer, 139(8), 082004.

Kumlutas, D., & Tavman, I. H. (2006). A numerical and experimental study on thermal conductivity of particle filled polymer composites. *Journal of thermoplastic composite materials*, *19*(4), 441-455.

Mark, J. E. (Ed.). (2007). *Physical properties of polymers handbook* (Vol. 1076, p. 825). New York: Springer.

Metropolis, N., Rosenbluth, A. W., Rosenbluth, M. N., Teller, A. H., & Teller, E. (1953). Equation of state calculations by fast computing machines. *The journal of chemical physics*, *21*(6), 1087-1092.

Naveira-Cotta, C. P., Cotta, R. M., & Orlande, H. R. (2011). Inverse analysis with integral transformed temperature fields: Identification of thermophysical properties in heterogeneous media. International Journal of Heat and Mass Transfer, 54(7-8), 1506-1519.

Neal, R. M. (2011). MCMC using Hamiltonian dynamics. *Handbook of markov chain monte carlo*, *2*(11), 2.

Torres, M. P. Determinação de propriedades térmicas em problemas de condução de calor por inferência Bayesiana com o método de Monte Carlo Hamiltoniano. 2018. 87 f. Dissertação (Mestrado em Modelagem Computacional) – Instituto Politécnico, Universi-dade do Estado do Rio de Janeiro, Nova Friburgo, 2018.

Torres, M. P., da Silva, G. R., Stutz, L. T., Knupp, D. C., Silva Neto, A. J., Application of the Hamiltonian Monte Carlo method for thermal properties estimation in thin plates. III Simposio Internacional de Modelación aplicada a la Ingeniería (MAI 2018), 2018, La Habana, 2018.

Wang, X. M., Zhang, L. S., Yang, C., Liu, N., & Cheng, W. L. (2019). Estimation of temperature-dependent thermal conductivity and specific heat capacity for charring ablators. *International Journal of Heat and Mass Transfer*, *129*, 894-902.

8. RESPONSIBILITY NOTICE

The authors are the only responsible for the printed material included in this paper.